Folding and Assembly of Lambda Cro Repressor Dimers Are Kinetically Limited by Proline Isomerization†

W. John Satumba and Michael C. Mossing*

Department of Chemistry and Biochemistry, University of Mississippi, University, Mississippi 38677

Received September 3, 2002; Revised Manuscript Received October 10, 2002

ABSTRACT: Cro binds to operator sites in lambda DNA as a dimer. Dimerization of this small repressor protein is weak, however, and proline residues in the dimer interface suggest that folding and assembly of active repressors may be complex. Cro and selected variants have been studied by circular dichroism and fluorescence. Fluorescent probes include a unique tryptophan residue in the dimer interface and extrinsic resonance energy transfer probes that monitor dimerization. Both folding and unfolding are characterized by two distinct kinetic phases. Fast processes that are complete within the 5−10 ms dead time of stopped flow experiments account for the majority of the change in the CD signal and abrupt changes in both tryptophan fluorescence and energy transfer. The slow phases show all the hallmarks of proline isomerization. The rates of the slow phases are between 0.005 and 0.02 s^{-1}, are relatively independent of protein and denaturant concentration, display activation energies of 20 kcal/mol, and are accelerated by the peptidyl−prolyl isomerase SlyD. Although CD measurements indicate that more than 70% of the secondary structure is regained in the refolding burst phase, intermolecular fluorescence resonance energy transfer experiments indicate that less than 25% of these subunits are assembled into dimers. Full folding and dimerization requires isomerization of the non-native prolyl isomers over hundreds of seconds.

Cro repressor dimers bind to operator sequences in bacteriophage λ DNA to seal the fate of a host cell that is bound for destruction after infection or induction of a lysogen (*1*). In both situations, the patterns of gene regulation and the observed switching probabilities suggest that the production of the active Cro repressor may be a relatively slow process. The developmental decision either to lysogenize or to lyse its host cell has classically been described as a competition between Cro and the lambda repressor cI (*2*). cI and Cro are repressors whose affinities for operator DNA are similar in vitro (*3*). In the program of λ early gene expression, Cro is produced from the very first transcript, while cI is produced only after three sequential rounds of transcription, translation, and protein function (*1*). The first round produces the transcription antiterminator N. N allows for a second round of transcription of the cII and cIII genes. And finally, cII activates a third round of transcription of cI. How is it that Cro has not already won the competition by the time cI is transcribed? In the case of the induction of lysogens, the autoregulatory circuit established by cI (and opposed by Cro) is remarkably stable (*4*, *5*). How is it that inevitable fluctuations in the level of cI do not lead to sporadic Cro transcripts, bursts of Cro synthesis, and premature induction? Both of these puzzles may be resolved if Cro is unusually slow to fold and assemble into an active repressor.

The Cro repressor of bacteriophage lambda is among the simplest DNA binding proteins. Cro recognizes lambda operator sequences as a homodimer of 66-residue subunits. The biophysical properties and structure of Cro (Figure 1) suggest that the kinetics of folding and dimer assembly might be important for its regulatory function. Equilibrium dissociation constants for Cro dimers in the absence of DNA have been reported to range from 0.3 (*6*) to 3 μM (*7*). In contrast, Cro dimers achieve half-saturation of operator DNA at nanomolar concentrations of subunits (*3*, *8*, *7*), where in the absence of DNA most subunits would be monomeric. At physiological concentrations of Cro subunits, well below the dimer dissociation constant, the DNA binding reaction is coupled to dimer assembly. Additional evidence that unfavorable assembly of dimers at low concentrations detracts from DNA binding affinity comes from single-chain dimers of Cro whose net affinity for DNA has been enhanced by more than 100-fold compared to that observed for unlinked subunits (*9*). Dimerization contacts between the two 66-residue subunits are located primarily between the third β-strands of each subunit (*10*). Residues A52, E54, K56, and F58 form backbone hydrogen bonds with their counterparts from the opposite subunit to join the three β-strands in each subunit into a six-stranded antiparallel sheet in the dimer. F58 anchors the dimer interface. In reaching across the dimer interface to pack against residues from the opposite subunit, F58 is responsible for 180 Å^2 of a total of 680 Å^2 of accessible surface buried in the dimer interface. F58 is flanked by two prolines. In the native dimer, the K56−P57 peptide bond is in the trans configuration while the F58−P59 bond is cis. Figure 1C shows the backbone configuration for residues 56−59 that is common to Cro and its single-tryptophan variant Cro F58W (see below).

We have used three variants of Cro to study the folding and dimer assembly process. Two single-residue substitu-

† This research was supported by Grant MCB-9874613 from the National Science Foundation.

* To whom correspondence should be addressed: Department of Chemistry and Biochemistry, University of Mississippi, University, MS 38677. E-mail: mmossing@olemiss.edu. Fax: (662) 915-7300.

10.1021/bi026777h CCC: $22.00
Published on Web 11/09/2002

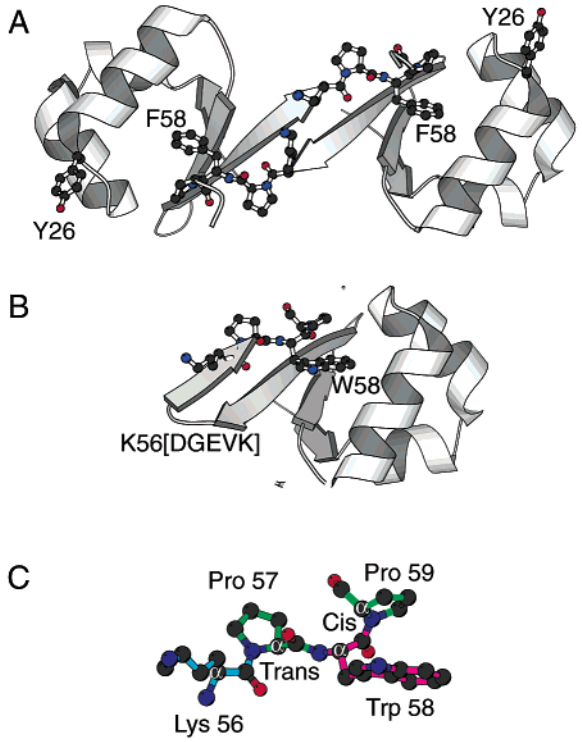

FIGURE 1: Structure of Cro and variants. (A) Ribbon diagram of the wild-type Cro dimer structure (*10*) with residues 26 and 56−59 shown as ball-and-stick models. Note that although wild-type (wt) Cro has 66 residues only the first 61 residues are visible in the crystal structure. (B) Ribbon diagram of the monomeric variant Cro K56[DGEVK] F58W (*18*). (C) Detail of the K56-P57-W58-P59 tetrapeptide from the structure in panel B. α-Carbons are labeled to show the trans and cis peptide isomers. This figure was drawn with Molscript (*34*).

tions, Y26C (*11*) and F58W (*12*), each stabilize the folded structure of Cro while introducing unique cysteine and tryptophan side chains, respectively. Tyrosine 26 is located far from the dimer interface in the turn of the helix−turn−helix DNA binding unit. Its exposure on the protein surface allows it to make direct contact with the DNA. The distance between the Y26 α-carbons in the Cro dimer pictured in Figure 1A is 40 Å, a distance that is convenient for resonance energy transfer studies (*13*). Many amino acid substitutions at position 26 are compatible with the folded structure of Cro, and in fact, most substitutions (including Y26C) stabilize Cro against denaturation (*14*). Although F58 is the key residue in the dimer interface, its environment is somewhat variable in different crystal structures (*10*, *15*−*17*). Substitution of F58 with tryptophan makes a protein that is more stable, while maintaining a similar structure (*18*) and affecting DNA binding only slightly (*7*). The F58W (Figure 1B,C) mutation provides a unique intrinsic fluorescent probe, as there are no tryptophans in wild-type Cro. Engineered monomeric variants of Cro contain the five-residue insertion/duplication K56[DGEVK] (*19*). The first two residues (DG) form the apex of a *β*-hairpin, while the remaining three residues (EVK) reiterate the connectivity normally supplied by the other subunit in the dimer. Figure 1B shows the structure of the double mutant Cro K56[DGEVK] F58W (*18*). The structures of the region surrounding residue 58 in the monomer and dimer are similar (*17*, *18*).

Interconversion of the cis and trans configurations of the peptide bonds that precede proline residues is a slow process (*20*). Work on unstructured pentapeptides (*21*) makes it possible to predict kinetic and thermodynamic properties of X−Pro peptide bonds in the unfolded state. SlyD is a peptidyl−prolyl isomerase (*22*) that was first identified as a host mutant that prevented lysis by bacteriophage Phi X174 (*23*). Several groups have purified SlyD, sometimes inadvertently by virtue of its naturally histidine rich C-terminus (*24*). Given its apparent role in the development of another *Escherichia coli* phage, we have tested its ability to accelerate the folding of Cro.

EXPERIMENTAL PROCEDURES

Buffers and Reagents. KP200 buffer is 20 mM potassium phosphate, 0.2 M potassium chloride, and 0.1 mM EDTA (pH 7). All experiments were conducted in KP200 unless otherwise indicated. Urea stocks were made from ultrapure urea purchased from ICN Biomedicals. Concentrations were verified by refractive index measurements on a Bausch and Laumb refractometer (*25*). 5-({[(2-Iodoacetyl)amino]ethyl}-amino)naphthalene-1-sulfonic acid (IAEDANS),[1] 6-iodoacetamidofluorescein (IAF), and tris(2-carboxyethyl)phosphine hydrochloride (TCEP) were purchased from Molecular Probes.

Protein Purification and Characterization. The two tryptophan variants (F58W dimer and the engineered monomer), Y26C, and wild-type Cro were all expressed and purified as previously described (*12*). The Cro Y26C/F58W double mutant was constructed by joining the N- and C-terminal parts of the singly mutant genes via an intervening *Bam*HI site (G. L. Bidwell, unpublished results). Protein purity was estimated to be >95% by SDS gel electrophoresis and Coomassie staining. Electrospray mass spectra were obtained on a Bruker BioApex 3T FTMS instrument using direct injection with an Analytica source. The masses of wt Cro, Cro F58W, and Cro Y26C were determined to be 7364, 7403, and 7302, respectively. Each is within 4 mass units of the mass predicted from the protein sequence. The mass of Cro Y26C/F58W was determined to be 7425, a mass that is consistent with a protein−2-mercaptoethanol adduct. Protein concentrations were determined by UV absorbance at 280 nm using extinction coefficients of 2660 M^{-1} cm^{-1} for Cro Y26C, 3990 M^{-1} cm^{-1} for wt Cro, 9590 M^{-1} cm^{-1} for both Cro F58W and Cro K56[DGEVK] F58W, and 8260 M^{-1} cm^{-1} for Cro Y26C/F58W (*7*).

Labeling of the Y26C mutant proteins using IAEDANS and IAF was carried out using a standard protocol as suggested by the supplier. Protein was reduced with TCEP and reacted with a 10-fold excess of either IAEDANS or IAF dissolved in dimethylformamide, for 1 h at room temperature or overnight at 4 °C. Excess iodoacetamide reagent was quenched with a 5-fold excess of 2-mercaptoethanol. Reaction mixtures were dialyzed extensively to remove excess dye, loaded onto a 1 mL Hitrap-SP cation exchange column (Pharmacia), and eluted with a linear gradient of 0 to 1 M NaCl in 20 mM potassium phosphate (pH 7). Concentrations of the dyes in the purified protein

[1] Abbreviations: wt, wild-type; IAEDANS, 5-([{(2-iodoacetyl)-amino]ethyl}amino)naphthalene-1-sulfonic acid; IAF, 6-iodoacetamidofluorescein; TCEP, tris(2-carboxyethyl)phosphine hydrochloride; NBS, *N*-bromosuccinimide; CD, circular dichroism; FRET, Förster resonance energy transfer.

fractions were calculated using an ϵ_{336} of 5600 M^{-1} cm^{-1} for IAEDANS and an ϵ_{490} of 61 000 M^{-1} cm^{-1} (at pH 7) for IAF. The concentrations of purified labeled proteins were determined either from the residual absorbance at 280 after subtracting out the dye contribution or with the Bradford assay. Purified fractions of both IAEDANS- and IAF-labeled Cro Y26C contained >95% singly labeled subunits. Electrospray mass spectra of labeled proteins showed molecular weights of 7617 (AE) and 7690 (Fl) and no detectable peaks at the native molecular weight of Y26C. The double mutant protein Cro Y26C/F58W was labeled in the same way.

The peptidyl−prolyl isomerase SlyD was purified from *E. coli* RY3131 (*26*). Cells were grown in LB medium at 37 °C to an A_{600} of 1. IPTG was added to a final concentration of 1 mM, and growth was continued for 3 h. Cells were pelleted by centrifugation, resuspended in 50 mM Tris, 100 mM NaCl, 15% sucrose, 1 mg/mL lysozyme, and 1 mM PMSF, and lysed by a freeze−thaw osmotic shock procedure. The crude lysate was centrifuged for 30 min at 15000*g*. The supernatant from 250 mL of culture was filtered through a 0.45 μm filter and applied to a 6 mL Ni−NTA column (Qiagen). The column was washed with 50 mM Tris, 300 mM NaCl, and 1 mM BME and eluted with a step gradient of 250 mM imidazole. Fractions containing SlyD were pooled, diluted into 20 mM phosphate buffer (pH 7), and loaded on a 1 mL MonoQ column which was developed with a linear gradient of NaCl from 0 to 1 M over 20 column volumes. SlyD eluted at 0.4 M NaCl. Thr purity was estimated to be >90% by SDS−PAGE.

Equilibrium Denaturation. CD and fluorescence signals were monitored as a function of urea concentration. CD was observed at 222 nm in an AVIV 202SF instrument with an automated double-syringe titrator. Two solutions were made with an identical buffer composition, pH, and protein concentration but differing urea concentrations. Typically, titrations were accomplished by addition of small aliquots of protein in 9−10 M urea to an identical solution that began with no urea. Serial removal and addition of additional aliquots of the high-denaturant solution generated the range of urea concentrations needed for the denaturation curve. The equilibration time for each concentration was 10 min, and the integration time was set at 30 s. Fluorescence titrations were carried out manually in a 1 cm square cuvette with a magnetic stirrer in a JY-Horiba Fluoromax 3 spectrofluorometer with excitation at 280 nm and emission at 342 nm. The integration time was also 30 s. Temperatures in both instruments were regulated at 25 °C.

Kinetic Experiments. The native protein was diluted into high concentrations of urea to initiate unfolding. Typical final urea concentrations were 2−6 M for Cro and Cro F58W and 2−8 M for the monomeric variant Cro K56[DGEVK] F58W. Kinetics were monitored in both the stopped-flow and manual mixing mode. Protein samples were denatured in 6−8 M urea for at least 2 h and equilibrated at 25 °C. For stopped-flow and manual mixing kinetics, urea-denatured states were refolded to final urea concentrations of 0.5−4 M using KP200. In manual mixing experiments, instrument settings were exactly as described above for equilibrium experiments to allow for direct comparison of signals. Stopped-flow experiments were performed with an AVIV stepper motor-driven stopped-flow unit or an Applied Photophysics RX.2000 rapid mixing accessory. In both cases, stopped-flow dead times were determined using NBS and *N*-acetyltryptophanamide (*27*) under the same solution conditions as the Cro unfolding and refolding experiments. Dead times were determined to be 10−15 ms for the Applied Photophysics unit and 5−10 ms for the AVIV SF202 unit.

Catalysis of Refolding by the PPIase SlyD. Cro F58W (120 μM) in potassium phosphate (20 mM) was acidified to pH 2 with HCl and equilibrated for at least 2 h. SlyD at concentrations from 1 to 20 μM was pre-equilibrated in 100 mM potassium phosphate (pH 7). The acid-denatured Cro F58W was then diluted into either 100 mM potassium phosphate (pH 7) or a SlyD solution to a final concentration of 20 μM. Tryptophan fluorescence was measured as described above. Since SlyD has no tryptophan residues, its contribution to the fluorescence signal was minimal.

Fluorescence Resonance Energy Transfer Experiments. Excitation and emission spectra for pure Cro Y26C−AEDANS donor, pure Cro Y26C−AF acceptor, and equimolar mixtures of the donor and acceptor were obtained on a Fluoromax3 spectrofluorometer. Equimolar mixtures of the Cro Y26C−AEDANS and Cro Y26C−AF complexes were denatured, and refolding was initiated as described above. The final total subunit concentration was 1 μM. Emission wavelength scans with excitation set at 336 nm with a resolution of 1 nm and an integration time of 0.1 s were initiated within 10 s of mixing. Immediately thereafter, scans were repeated with the excitation wavelength set to 430 nm, where the donor absorbance is negligible.

Data Analysis. Kinetic and equilibrium data were fit using nonlinear least-squares routines in Matlab. All kinetic data fit well to a single-exponential equation. Equilibrium data were fit assuming linear dependencies for the spectroscopic signals from the folded state (S_f) and the unfolded state (S_u) and the free energy (ΔG) on the concentration of denaturant. For each individual data set, a total of six parameters, a slope and an intercept for each of the variables (S_f, S_u, and ΔG), were determined in the fitting process (*28*). In some cases, m and ΔG values were fit globally for multiple data sets, while determining optimal baseline parameters locally for each data set.

For both Cro dimers and engineered monomers, the observed signal was fit according to the following relationship between fraction unfolded (f_u) and S.

$$S = S_f(1 - f_u) + S_u f_u$$

For the concerted dimer dissociation−unfolding model $F_2 \rightleftarrows 2U$, f_u depends on the total protein concentration

$$f_u = \frac{-K + \sqrt{K^2 + 8PtK}}{4Pt}$$

for the monomer unfolding model $F \rightleftarrows U$, f_u is independent of the total protein concentration.

$$f_u = \frac{K}{1 + K}$$

In both cases, $\Delta G = -RT \ln K$.

In all cases, errors in fitted parameters are reported as 95% confidence intervals.

RESULTS

We have investigated refolding from three different denatured states, acid-denatured at pH 2, 8 M urea, and 6 M

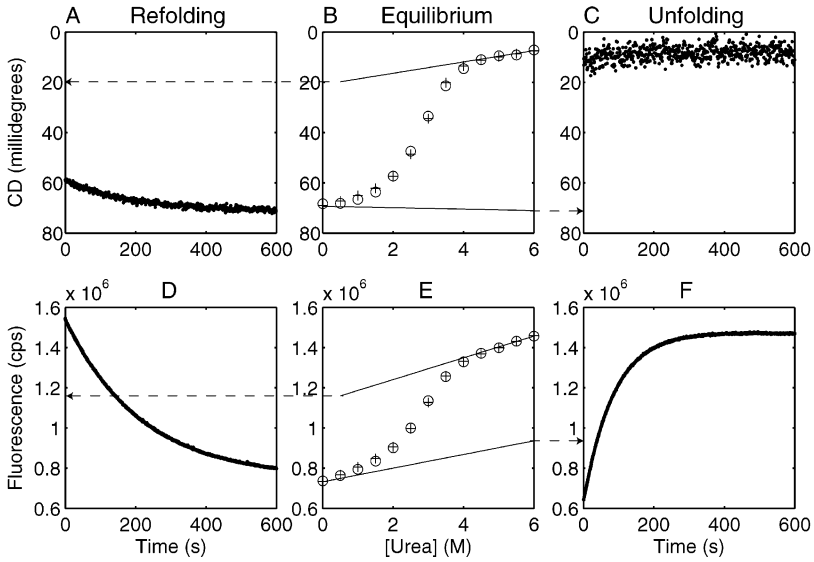

FIGURE 2: Cro F58W folding and unfolding. Discrepancies between equilibrium fluorescence and kinetic burst phase signals indicate the presence of folding and unfolding intermediates. Circular dichroism (A−C) and fluorescence (D−F) of a 10 μM solution of the single-tryptophan variant Cro F58W. Panels A and D show the time evolution of the spectroscopic signals after the initiation of refolding by dilution from 6 to 0.5 M urea. Panels B and E show equilibrium signals as a function of urea concentration. Solid lines represent the folded and unfolded baseline signals derived from global fits of the CD and fluorescence data. Panels C and F show the time evolution of the spectroscopic signals after the initiation of unfolding by dilution into 6 M urea. In all cases, the final protein concentration was 10 μM. Dashed arrows depict the initial spectroscopic signal expected in kinetic experiments based on linear extrapolation of the folded and unfolded baselines.

guanidine hydrochloride. Similar kinetics were observed upon refolding from each of the three states. The observed amplitudes and rates of refolding processes were independent of the denaturant concentration used to unfold the protein over the range of 6−8 M urea, 4−6 M guanidine hydrochloride, and pH 1.8−2.1. Analysis of equilibrium denaturation with urea is more straightforward than with either guanidine hydrochloride or pH. Urea denaturation yields linear pre- and post-transition baselines. Guanidine hydrochloride (and other salts, H. Maity and M. Eftink, unpublished results) appears to stabilize the native state at low concentrations and results in nonmonotonic pretransition baselines. Likewise, quenching of tryptophan fluorescence at low pH precludes simple analysis of the acid-denatured baseline. For these reasons, urea was chosen as the primary denaturant for studying the relationship between equilibrium and kinetic signals. Refolding was studied in two quaternary structure contexts, that of the wild-type 66-residue dimer and in the context of the engineered monomeric insertion mutant Cro K56[DGEVK]. In all cases, the results obtained with Cro K56[DGEVK] F58W were independent of protein concentration, as expected for an exclusively monomeric protein. Somewhat surprisingly, the results with Cro and Cro F58W were also relatively independent of protein concentration. In the range of 1−20 μM, neither the rates nor the relative amplitudes of the kinetic phases that we detected varied by more than 2-fold. Observed folding and unfolding rates were similarly independent of urea concentration, varying less than 2-fold over the range of 0.5−6 M urea.

For wild-type Cro, unfolding and refolding can be followed by circular dichroism, while for Cro F58W, fluorescence of the unique tryptophan residue provides an additional spectroscopic signal. Figure 2 shows representative equilibrium and kinetic profiles for Cro F58W at a subunit concentration of 10 μM. The fact that the burst phase fluorescence of both the unfolding and refolding traces is outside the range of equilibrium data indicates that intermediates are populated in both kinetic processes. Panel B shows an equilibrium denaturation profile monitored by CD at 222 nm. Panel E shows the tryptophan fluorescence signal obtained at 342 nm after excitation at 280 nm under the same solution conditions. CD and fluorescence data sets were fit globally to a two-state unfolding model ($F_2 \rightleftarrows 2U$) to give common $\Delta G°(H_2O)$ and m values and data-set specific baseline parameters. The results of the fits are illustrated graphically in panels B and E. For these particular data sets, $\Delta G°_{H_2O} = -11.4 \pm 0.4$ kcal/mol and $m = 1.71 \pm 0.12$ kcal/mol. Under these solution conditions, at Cro F58W subunit concentrations of $\geq$10 μM, the two-state dimer unfolding model provides good fits. Fitting of multiple data sets individually yields similar error ranges for $\Delta G°_{H_2O}$ and m.

Refolding kinetic traces shown in panels A and C show the evolution of CD and fluorescence signals with time after dilution of the protein from 6 M urea to 0.5 M urea at 25 °C. Arrows indicate the position of the signals predicted by linear extrapolation of the denatured equilibrium baseline to 0.5 M urea. In both cases, the initial signals that were detected were significantly different than predicted by linear extrapolation, indicating the presence of a refolding burst phase. The initial CD signal obtained in refolding experiments is consistent with recovery of 77 $\pm$ 5% of the native CD signal in the dead time of the experiment. Similar experiments performed with wt Cro also give a burst phase CD signal of 80 $\pm$ 5%, while experiments conducted with the Cro K56[DGEVK] F58W monomer show recovery of 95 $\pm$ 2% of the native CD in the burst phase (data not shown).

The initial fluorescence signal observed upon refolding is outside the range observed for the equilibrium denaturation of Cro F58W, and indicates the population of a distribution of protein conformers different from that observed under

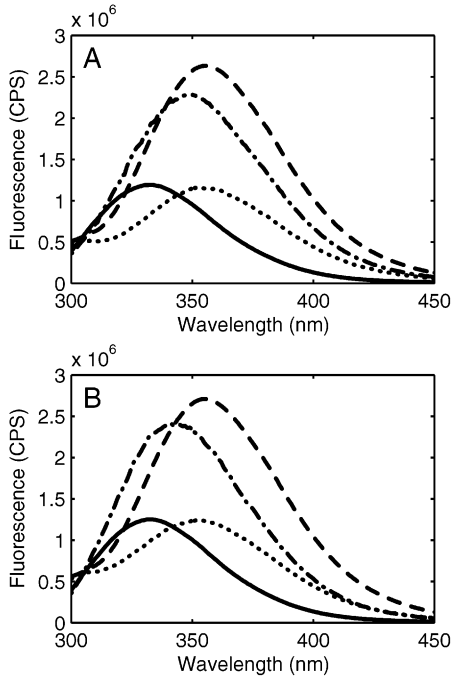

FIGURE 3: Tryptophan fluorescence spectra of folding intermediates. Fluorescence emission spectra of 5 μM Cro F58W (A) and the monomeric variant Cro K56[DGEVK] F58W (B). Excitation was at 280 nm. The solid lines are the spectra of the native proteins. The dotted line spectra were obtained immediately following transfer from 0 to 6 M urea. Dashed lines are the equilibrium spectra obtained in 6 M urea. Dotted−dashed line spectra were obtained immediately following transfer from 6 to 0.5 M urea.

equilibrium conditions. The slow recovery of the native CD and fluorescence signals can be fit with a single exponential with a similar rate constant of 0.005 ± 0.0005 s^{-1}. This rate constant is in the range expected for isomerization of the peptide bond that separates W58 from P59.

Kinetic traces in panels C and F of Figure 2 show the signal changes observed upon addition of 6 M urea to a solution of native Cro. Nearly all of the CD signal is lost in the dead time of the mixing experiment. The small amplitude of the CD signal and the noise inherent in the high-denaturant solution precluded a definitive kinetic analysis of the unfolding kinetics by CD. Tryptophan fluorescence shows a large amplitude kinetic phase with a rate of 0.012 ± 0.002 s^{-1}. As in the refolding experiment, the initial fluorescence signal is outside the range defined by the equilibrium signals. The rates and amplitudes of the kinetic phases observed by CD and fluorescence remained the same over the protein concentration range of 1−20 μM. In these manual mixing experiments, the lag time between protein dilution and data acquisition is on the order of 10 s. However, stopped-flow experiments with dead times of 5−10 ms show similar burst phase amplitudes (data not shown) and no detectable faster kinetic phases.

The unusual kinetic behavior of the tryptophan fluorescence signal observed at 342 nm and the slow rate of change in the signal prompted us to undertake a full spectral analysis of the intermediates that were observed. Figure 3 shows fluorescence spectra taken under native conditions (0 M urea), under denatured conditions (6 M urea), and within the first 20 s after a rapid dilution from 6 to 0.5 M and after dilution from 0 to 6 M urea. The F58W variant was studied in both the context of the wild-type protein and the K56-[DGEVK] insertion mutant which creates an obligatory monomer. In both the native and equilibrium-denatured states, the steady state fluorescence of the two proteins is almost identical as expected from the similarity of the tryptophan environments in their crystal structures (*18*). The integrated intensity of the fluorescence emission spectra of the denatured state is 2.65-fold higher than that of the native state, and the center of mass of the spectrum shifts from 339 to 360 nm. Upon denaturation, fluorescence spectra acquired in the first 20 s after transfer to 6 M urea show nearly all of the red shift (center of mass is 357 nm) seen in the denatured state, but the total intensity increases by only 20−30%. The fluorescence intensity slowly builds to the denatured state with only slight changes in the shape or position of the spectral distribution. Since the far-UV CD signal has essentially reached its denatured end point at the start of the reaction, we interpret this fluorescence change to be due to direct interactions between W58 and P59, as the peptide bond that separates them isomerizes from the native all-cis isomer distribution to the equilibrium distribution of cis and trans isomers. Upon initiation of refolding to 0.5 M urea, again a rapid process results in a change in the spectral distribution of fluorescence emission, and the overall fluorescence decreases from 2.6 to 2.2 times that of the native state for both the monomer and the dimer. The initial fluorescence of the monomer is significantly shifted toward the wavelength distribution of the native protein. From an initial red shift of 20 Å between the native and denatured proteins, the initial refolding spectrum of the dimer shows a shift in the wavelength of maximal fluorescence of only 3 Å while the monomer shows an 11 Å shift toward the native state. The larger amplitude burst phase CD signal for the monomer insertion mutant and its more nativelike fluorescence spectrum indicate a greater level of folded structure for these folding intermediates.

Two hallmarks of proline isomerization reactions are a large activation energy and susceptibility to catalyis by peptidyl−prolyl cis−trans isomerase (PPIase). To determine whether the slow phase that we observe in refolding has a temperature dependence that is consistent with proline isomerization, we performed refolding studies at temperatures ranging from 10 to 30 °C. Cro F58W in 6 M urea was preequilibrated at the desired temperature and then diluted to 0.5 M urea as described above. Figure 4 shows kinetic traces obtained at five different temperatures. Analysis of the data yields an activation energy of 20.8 kcal/mol, a value commonly found for proline isomerization reactions (*21*). Figure 5 shows the effects of the PPIase SlyD on the refolding kinetics of Cro F58W. In the absence of SlyD, the observed first-order rate is 0.006 s^{-1}, as expected on the basis of observations of refolding from urea, but in the presence of 5 μM SlyD, the observed refolding rate is 0.014 s^{-1}. The observed first-order rate constant increases linearly with SlyD concentration over the range of 1−20 μM.

Experiments described thus far have shown that Cro refolds in two phases, a rapid phase that results in the recovery of ~70% of the native CD signal and a slow phase that we attribute to proline isomerization. Neither phase shows the dependence on protein concentration that is expected for a bimolecular dimerization step. We have used resonance energy transfer to determine the extent to which the species formed in the burst phase are dimeric. In a

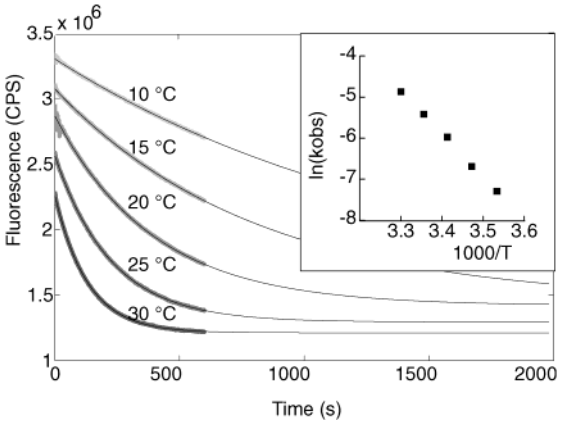

FIGURE 4: Temperature dependence of Cro F58W refolding which is consistent with proline isomerization. Tryptophan fluorescence was excited at 280 nm and emission monitored at 342 nm as a function of time. Experimental data points at five temperatures are indicated in gray, and single-exponential fits to the data are represented as thin black lines. The inset shows the observed first-order rate constants plotted against inverse temperature in an Arrhenius plot.

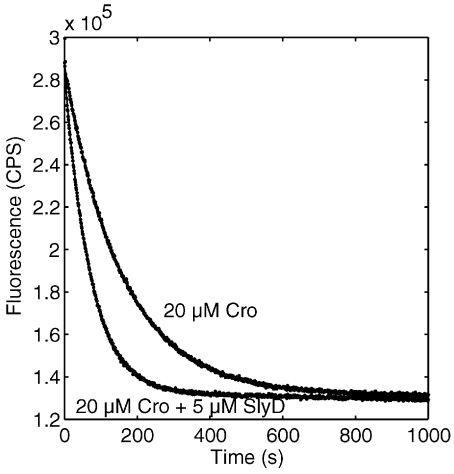

FIGURE 5: SlyD peptidyl−prolyl isomerase accelerates the slow refolding phase. Tryptophan fluorescence was excited at 280 nm and emission monitored at 342 nm as a function of time. Cro F58W was acid-denatured and refolded at a final concentration of 20 μM in 100 mM potassium phosphate or in the same buffer with 5 μM SlyD. Single-exponential fits to the data are plotted as thin solid lines.

population of subunits that have been separately labeled with either fluorescence donors or acceptors, energy transfer can occur only after the formation of heterodimers. If subunit mixing is random, and the distances between fluorescent probes are uniform in all dimers, then the energy transfer signal should be directly proportional to the number of dimers. Kinetic analysis of refolding experiments that monitor energy transfer shows the same single-exponential behavior and first-order rate constants as observed in the CD and tryptophan fluorescence experiments described above (data not shown). The initial fluorescence signals observed in stopped-flow and manual mixing experiments indicated that a significant FRET signal was present already in the burst phase. To quantify the extent of dimer formation in the burst phase, we again take advantage of the large difference in the time scales of the fast and slow phases and analyze complete fluorescence spectra. As described below, this allows for accurate quantitation of donor and acceptor

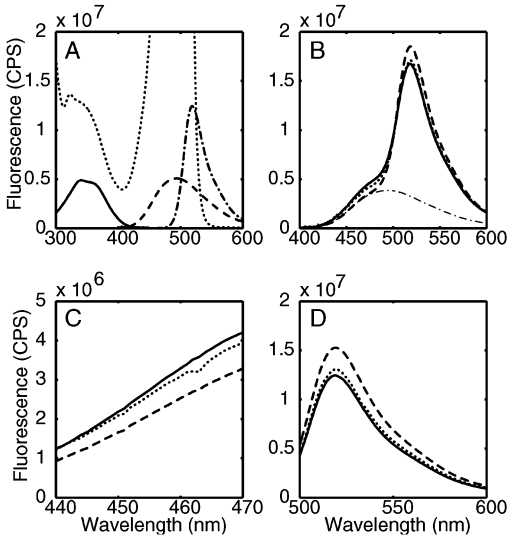

FIGURE 6: Dimerization analysis by intermolecular fluorescence resonance energy transfer. (A) Excitation spectra of separate solutions of donor (solid line, emission at 490 nm) and acceptor (dotted line, emission at 490 nm). Emission spectra of donor (dashed line) and acceptor (dotted−dashed line) both with 336 nm excitation. (B) Sum of the emission spectra of the donor and acceptor from panel A (solid line). Emission spectra of a 1:1 mixture of donor and acceptor at 20 s (dotted line) and 600 s (dashed line) and the calculated AEDANS contribution to the 600 s spectra (thin dotted−dashed line). (C) Expanded view of the 440−470 nm region from panel B showing the energy transfer effects on donor fluorescence in the absence of energy transfer (solid line) at 20 (dotted line) and 600 s (dashed line). (D) Acceptor contributions to the fluorescence in the 500−600 nm region in the absence of energy transfer (solid line) at 20 s (dotted line) and 600 s (dashed line).

contributions to the total fluorescence at the wavelengths where FRET is assessed. Analysis of complete spectra also allows a single sample to provide a direct comparison of the relative reduction in donor fluorescence and the enhancement of acceptor fluorescence due to energy transfer.

Fluorescence spectra of separate solutions of the Cro Y26C−AEDANS (donor) and Cro Y26C−AF (acceptor) complexes are shown in Figure 6A. The extinction coefficients at the absorbance maximum of the AEDANS donor ($\epsilon_{336} = 5600$) and AF acceptor ($\epsilon_{490} = 61\,000$ at pH 7) are quite different. Excitation scans were done with emission set at maxima of 490 nm for AEDANS and 520 nm for AF. For energy transfer experiments, donor fluorescence is excited at 336 nm and detected in the range of 440−470 nm where acceptor fluorescence is minimal. Acceptor fluorescence is also directly excited at 336 nm, and donor fluorescence contributes throughout the acceptor emission range, necessitating corrections in the analysis of acceptor emission after energy transfer. From the acceptor excitation spectrum, note that equivalent acceptor fluorescence signals can be obtained with 336 and 430 nm excitation, but that excitation at 430 nm does not excite donor fluorescence appreciably. The unique donor fluorescence with excitation at 336 nm and emission in the range of 440−470 nm and acceptor fluorescence excited at 430 nm and monitored at 520 nm were used as internal standards to measure acceptor energy transfer efficiency as described below.

Figure 6B shows three emission spectra obtained with excitation at 336 nm, and each is the average of three independent experiments. The solid line represents the sum

of the donor and acceptor emission spectra from panel A. Spectra obtained from an equimolar mixture of acceptor and donor subunits (total subunit concentration of 1 μM) were recorded at 20 s (dashed line) and 600 s (dotted line) after transfer from 6 to 0.5 M urea. Once a mixture of donor and acceptor has been refolded, the initial spectrum is slightly lower in magnitude than the sum of the donor and acceptor spectra in the region from 440 to 470 nm and slightly larger in magnitude than the sum of the spectra at wavelengths greater than 500 nm. Quantitation of donor energy transfer is straightforward. Since acceptor fluorescence is minimal in the 440−470 nm range (see Figure 6A), the reduction in the observed fluorescence in this wavelength range can be attributed to energy transfer. Panel C shows that between 10 and 20 s of refolding the donor fluorescence is reduced by 7% relative to the donor only spectrum and after 600 s by 24%. In this case, the burst phase FRET signal is 27% of that observed after the completion of refolding.

To quantify the extent of energy transfer to the acceptor, the following strategy was adopted (*29*). To account for changes in donor fluorescence, the signal observed in the 440−470 nm region of the spectrum of the mixture was extrapolated to estimate the donor contributions at wavelengths in the acceptor emission region. The thin dotted−dashed line in panel B shows such an extrapolation based on the shape of the donor only emission spectrum and the amplitude of the mixture spectrum at 440−470 nm. Panel D shows the acceptor signal that remains after subtracting out the residual donor contributions. This remaining acceptor signal has two components, direct fluorescence of the acceptor due to excitation at 336 nm and energy transfer. Two separate standards for direct excitation were used. The first is the acceptor only spectrum from panel A, shown as a solid line. In addition, an internal standard for direct fluorescein fluorescence was generated by exciting the mixture at 430 nm, a wavelength where the donor is not excited and the acceptor fluorescence is equivalent to that generated at 336 nm (see the excitation spectrum in panel A). In this case, internal and external standards give nearly identical estimates of 5.3 and 5.4% enhancement of the acceptor signal in the 20 s spectrum and 25.7 and 24.8% for the 600 s spectrum, respectively. These translate to 20.4 and 21.6%, respectively, of the total amplitude occurring in the burst phase. The fraction of dimers formed in the burst phase can thus be estimated to be between 20 and 30%. This is in contrast to the 70−80% recovery of the CD signal in the burst phase and points to a substantially folded monomeric intermediate. Stopped-flow analysis of refolding by FRET gave the same burst phase amplitudes. Like recovery of CD and tryptophan fluorescence signals, the initial dimerization reaction from the unfolded state is fast. Recent experiments with the double mutant Cro Y26C/F58W, similarly labeled with AF and AEDANS, give initial FRET signals of 51 ± 5% of the final FRET amplitude.

DISCUSSION

Our overall view of Cro unfolding is as follows. Upon transfer to urea, secondary structure is lost very rapidly. Far-UV CD, Trp fluorescence, and FRET signals all change within 10 ms. Given the short time required for this unfolding process, the native distribution of proline isomers (K56−trans-P57 and W58−cis-P59) is initially nearly 100% populated in the unfolded state (signified U_c^t in Scheme 1). Trp fluorescence alone reports on a slow process that occurs on the time scale of hundreds of seconds. We take this to be the slow isomerization of a homogeneous U_c^t population to a population of unfolded chains with the equilibrium distribution of cis and trans isomers at each peptidyl−prolyl bond (U_c^t, U_t^t, U_t^c, and U_c^c as illustrated in Scheme 1). The equilibrium distribution of isomers can be estimated using data for unstructured pentapeptides (*21*). Reimer et al. found that the equilibrium distributions of cis isomers in KP, FP, and WP dipeptides were 7, 23, and 37%, respectively. The K56−K57 peptide bond is expected to remain predominantly in the native trans configuration. In contrast, 63% of the W58−P59 peptide or 77% of the F58−P59 peptide is expected to convert from cis to trans. The most straightforward interpretation of the large amplitude change in tryptophan fluorescence on unfolding is that even in the unfolded state the cis isomer of the W58−P59 peptide bond results in quenching of W58 fluorescence, and this quenching is relieved as the majority of the 58−59 bonds are converted to the trans state. Sendak et al. (*30*) observed a similar effect on the unfolding of the Y92W mutant of ribonuclease A. This mutant also results in a W−cis-Pro peptide bond in the native state. Relaxation to an equilbrium distribution of cis and trans isomers should go as the sum of the forward and reverse rates. Again on the basis of the data of Reimer et al. (*21*) for the WP peptide, $k_{c\rightarrow t} = 0.0065\ s^{-1}$ and $k_{t\rightarrow c} = 0.0039\ s^{-1}$, giving an expected relaxation rate of ~0.01 s^{-1} at 25 °C. The observed rate constant for the slow unfolding phase in both the monomer and dimer contexts is 0.014 ± 0.002 s^{-1}.

Scheme 1: Proposed Folding, Isomerization, and Assembly Mechanism for Cro Dimers

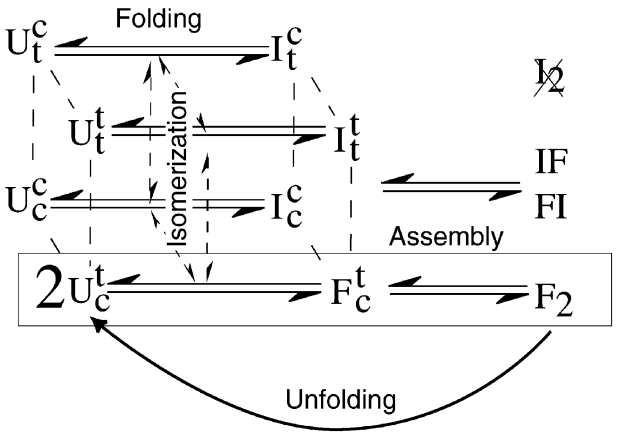

Upon initiation of refolding from an equilibrium distribution of unfolded chains, the behavior of the population is heterogeneous. The subpopulation of chains with native proline isomers (boxed species in Scheme 1) has no barrier to folding. The magnitude of the CD signal recovered in the burst phase, however, indicates that in addition to those chains with native prolyl isomers (denoted F in Scheme 1) the majority of the chains with non-native isomers (I in Scheme 1) can still fold. In the case of the β-hairpin monomer, approximately 95% of the CD signal is recovered in the burst phase, perhaps indicating that only species containing the non-native cis isomer at positions 56 and 57 (U_t^c and U_c^c with a cumulative expected abundance of 7%)

preclude folding and that both W58−P59 peptide bond configurations are compatible with formation of native levels of helical structure. Among the dimeric proteins that have been studied, the level of CD signal formed in the burst phase is between 70 and 80% of the native signal. This fraction, too, is larger than the expected fraction of native prolyl isomers (~21% for wt Cro and ~35% for the F58W protein). Thus, for the monomeric variant and both the wt and F58W dimers, we have a population of folding intermediates which achieve substantial secondary structure prior to peptide bond isomerization to the native configuration.

The initial amplitude of the fluorescence resonance energy transfer signal for a mixture of the Cro Y26C−AEDANS and Cro Y26C−AF complexes is 24 ± 5% of the FRET efficiency obtained at equilibrium. The primary conclusion to be drawn is that Cro subunits do not have to dimerize to fold. The proline isomer requirements for dimerization are now considered. The most restrictive scenario would be that dimer formation would require native proline configurations on both subunits (all dimers would be of the type indicated F_2 in Scheme 1). In this case, encounters in which either chain contained a non-native proline configuration would be unproductive and dimerization competent chains would be free to continue their search for competent partners. The proportion of subunits that are able to dimerize initially in this scenario would mirror the level of native proline configurations in the denatured state, 21% for wt Cro or 35% for Cro F58W. A second possibility is that a native proline configuration would be required on only one of the two chains required for dimer formation (IF, FI, and F_2 would all be potential dimers). In this scenario, a larger fraction of the total subunit population could be involved in dimerization initially. If wt Cro subunits were assorted randomly, F_2 dimers would be found at a frequency of 4.4% (0.21×0.21), while FI configurations would be more frequent at 33% ($2 \times 0.21 \times 0.79$) for a total potential dimer population of 37%. With the higher proportion of native cis isomers in Cro F58W, the expected frequencies would be 12% F_2 and 45% FI for a total of 57%. Finally, in the least restrictive case, all subunits could associate (I_2 could also dimerize). We do not favor this possibility. At a minimum, the stability of the I_2 dimer must be much less than those of the FI or F_2 dimers because the majority of the FRET amplitude is attained only after proline isomerization. It should be noted that the isomer fractions and dimer probabilities calculated above represent the potential pools of subunits available for dimerization and thus the maximal number of dimers that could be expected in each case. Of course, lower dimerization free energies for non-native interfaces would reduce the actual fraction of dimers formed from these maximal estimates.

The initial FRET signal that we observe for Cro Y26C in refolding experiments (24 ± 5%) is right at the top of the range expected if two native proline configurations were required for dimerization. The higher initial FRET signal observed for the Cro Y26C/F58W dimers (51 ± 5%) is beyond the range predicted if only F_2 dimers are stable. Our data suggest that having one native isomeric configuration between the two subunits is sufficient for dimerization. If the majority of the dimers formed initially have only half of a properly configured dimer interface, this raises an interesting question concerning DNA binding. Since K56 makes contacts with the DNA in the Cro−operator complex and F58 is near the protein−DNA interface (*15*), it seems likely that fully native dimers will be required for operator recognition. Allowing for formation of mixed dimers with only one native C-terminus would reduce the initial number of repressors that are able to bind operator DNA.

Some caution should be exercised in the interpretation of these steady state FRET intensities. Changes in the distance between the two probes that accompany the maturation of the proposed intermediate dimers to the native dimer could also contribute to time-dependent changes in FRET. The distance between Y26 α-carbons in the native Cro dimer is 40 Å, slightly less than the Förster radius reported for the fluorescein−IAEDANS pair [46 Å (*13*)], making energy transfer sensitive to relatively modest changes in distance in this range. For example, the 70% efficiency calculated for an R of 40 Å would increase to 90% if R were 30 Å and decrease to 38% if R were 50 Å. FRET lifetime measurements may be able to resolve the ambiguity between distance and occupancy effects.

It may be useful to consider the Cro subunit as two subdomains. The larger N-terminal subdomain contains the helix−turn−helix unit and the bulk of the globular structure of the protein, while the smaller C-terminal subdomain consists of residues primarily involved in intermolecular interactions in the dimer interface (the β3 strand and Pro-Phe-Pro cluster). Our working model is that the N-terminal subdomain folds partially even in the absence of the Pro-Phe-Pro cluster. Association between the partially or transiently folded N-terminal subdomain and the Pro-Phe-Pro cluster from a separate subunit results in dimerization. In the case of the β-hairpin monomer, Cro K56[DGEVK] F58W, the Pro-Trp-Pro cluster is retained intramolecularly by the inserted hairpin sequence and even in the trans state can promote folding. It remains to be demonstrated whether similar intramolecular interactions are possible in folded monomers of the wild-type subunit. Recent experiments on subunit exchange in the native state (H. Jia, unpublished results) indicate that the association rate of Cro Y26C donor and acceptor monomers that are in equilibrium with dimers may be orders of magnitude slower than that inferred here from FRET refolding measurements. If interactions between the two subdomains can occur in both monomeric and dimeric contexts, substantial barriers to exchange may exist. Similar behavior has recently been demonstrated for several "domain-swapped" (*31*) systems, notably, the cks cell cycle control proteins p13suc (*32*) from *Schizosaccharomyces pombe* and ckshs1 and ckshs2 (*33*) from humans. In these proteins as in Cro, a Pro-X-Pro motif appears to control the equilibrium and kinetics of exchange between monomers and dimers.

Refolding of Cro dimers is characterized by a very rapid collapse process followed by slow proline isomerization. The rate of the slow phase is relatively unaffected by protein or denaturant concentration, but does depend on temperature and proline isomerase activity as expected. The slow rate of assembly of dimers may be important for the dynamic control characteristics of the lambda genetic switch. Future studies of the effects of DNA on assembly rates and on the rates of folding and assembly in vivo will address this question.

ACKNOWLEDGMENT

We thank Dr. Ryland Young of Texas A&M University (College Station, TX) for the kind gift of the SlyD expression plasmid, Ibrahim Al-Duraibi for purification of SlyD, Dr. Chuck Dunbar of the Cochran Center for Natural Product Research for mass spectroscopy, Dr. Maurice Eftink for use of his CD instrument, and Gene L. Bidwell III for construction and purification of the Cro Y26C/F58W double mutant protein.

REFERENCES

1. Ptashne, M. (1992) *A genetic switch: phage lambda and higher organisms*, 2nd ed., Blackwell Scientific Publications, Cambridge, MA.
2. Johnson, A. D., Poteete, A. R., Lauer, G., Sauer, R. T., Ackers, G. K., and Ptashne, M. (1981) *Nature 294*, 217−223.
3. Darling, P. J., Holt, J. M., and Ackers, G. K. (2000) *J. Mol. Biol. 302*, 625−638.
4. Aurell, E., Brown, S., Johanson, J., and Sneppen, K. (2002) *Phys. Rev. E: Stat., Nonlinear, Soft Matter Phys. 65*, 051914.
5. Little, J. W., Shepley, D. P., and Wert, D. W. (1999) *EMBO J. 18*, 4299−4307.
6. Darling, P. J., Holt, J. M., and Ackers, G. K. (2000) *Biochemistry 39*, 11500−11507.
7. Jana, R., Hazbun, T. R., Mollah, A. K., and Mossing, M. C. (1997) *J. Mol. Biol. 273*, 402−416.
8. Takeda, Y., Sarai, A., and Rivera, V. M. (1989) *Proc. Natl. Acad. Sci. U.S.A. 86*, 439−443.
9. Jana, R., Hazbun, T. R., Fields, J. D., and Mossing, M. C. (1998) *Biochemistry 37*, 6446−6455.
10. Ohlendorf, D. H., Tronrud, D. E., and Matthews, B. W. (1998) *J. Mol. Biol. 280*, 129−136.
11. Pakula, A. A., and Sauer, R. T. (1989) *Proteins 5*, 202−210.
12. Mollah, A. K., Aleman, M. A., Albright, R. A., and Mossing, M. C. (1996) *Biochemistry 35*, 743−748.
13. Wu, P., and Brand, L. (1994) *Anal. Biochem. 218*, 1−13.
14. Pakula, A. A., and Sauer, R. T. (1990) *Nature 344*, 363−364.
15. Albright, R. A., and Matthews, B. W. (1998) *J. Mol. Biol. 280*, 137−151.
16. Albright, R. A., Mossing, M. C., and Matthews, B. W. (1998) *Protein Sci. 7*, 1485−1494.
17. Albright, R. A., Mossing, M. C., and Matthews, B. W. (1996) *Biochemistry 35*, 735−742.
18. Rupert, P. B., Mollah, A. K., Mossing, M. C., and Matthews, B. W. (2000) *J. Mol. Biol. 296*, 1079−1090.
19. Mossing, M. C., and Sauer, R. T. (1990) *Science 250*, 1712−1715.
20. Fischer, G. (2000) *Chem. Soc. Rev. 29*, 119−127.
21. Reimer, U., Scherer, G., Drewello, M., Kruber, S., Schutkowski, M., and Fischer, G. (1998) *J. Mol. Biol. 279*, 449−460.
22. Hottenrott, S., Schumann, T., Pluckthun, A., Fischer, G., and Rahfeld, J. U. (1997) *J. Biol. Chem. 272*, 15697−15701.
23. Roof, W. D., Horne, S. M., Young, K. D., and Young, R. (1994) *J. Biol. Chem. 269*, 2902−2910.
24. Roche, E. D., and Sauer, R. T. (2001) *J. Biol. Chem. 276*, 28509−28515.
25. Pace, C. N. (1986) *Methods Enzymol. 131*, 266−280.
26. Roof, W. D., Fang, H. Q., Young, K. D., Sun, J., and Young, R. (1997) *Mol. Microbiol. 25*, 1031−1046.
27. Peterman, B. F. (1979) *Anal. Biochem. 93*, 442−444.
28. Santoro, M. M., and Bolen, D. W. (1988) *Biochemistry 27*, 8063−8068.
29. Clegg, R. M. (1992) *Methods Enzymol. 211*, 353−388.
30. Sendak, R. A., Rothwarf, D. M., Wedemeyer, W. J., Houry, W. A., and Scheraga, H. A. (1996) *Biochemistry 35*, 12978−12992.
31. Liu, Y., and Eisenberg, D. (2002) *Protein Sci. 11*, 1285−1299.
32. Rousseau, F., Schymkowitz, J. W., Wilkinson, H. R., and Itzhaki, L. S. (2001) *Proc. Natl. Acad. Sci. U.S.A. 98*, 5596−5601.
33. Seeliger, M. A., Schymkowitz, J. W., Rousseau, F., Wilkinson, H. R., and Itzhaki, L. S. (2002) *Biochemistry 41*, 1202−1210.
34. Kraulis, P. J. (1991) *J. Appl. Crystallogr. 24*, 946−950.

BI026777H